

# Magnetic Relaxation in Dynamically Heterogeneous Systems

Robert G. Bryant

*Chemistry Department  
University of Virginia  
Charlottesville, VA*

## Contents

|                      |     |
|----------------------|-----|
| I. Abstract          | 239 |
| II. Discussion       | 239 |
| III. Acknowledgments | 245 |
| IV. References       | 245 |

## I. Abstract

Nuclear magnetic spin-lattice relaxation in dynamically heterogeneous systems is generally coupled; that is, the rapidly moving liquid components do not relax independently of the rotationally immobilized or solid components. The consequences of this coupling are that the generally observable relaxation rates of the liquid components may not be interpreted using the standard theories of liquid spin relaxation, but the coupling also provides a pathway for reading the characteristics of the solid spin system by direct observation of only the liquid spin system. This fact provides a considerable opportunity for magnetic analysis of complex materials in such environments as process control, and also provides completely new opportunities for magnetic imaging. By application of an off-resonance preparation pulse one may impose the spin relaxation characteristics of the solid on the liquid, thereby providing solid component information in the liquid magnetic image.

## II. Discussion

Dynamically heterogeneous materials are common and include any system in which there is a liquid component in contact with a solid matrix. By solid we mean only that the rotational motion of the system is sufficiently slow that the intramolecular dipole-dipole couplings between the protons in the solid are not averaged by the molecular motion.

Typically this means that the motion is slow on the time scale of the order of 100  $\mu$ s or so. Many systems fall in this class of materials such as almost all biological tissues including plant and animal tissues, and many processed foods, heterogeneous catalytic materials, microporous media such as chromatographic materials, etc.

Magnetic resonance may provide both direct spectroscopic information from such materials as well as gross structural information based on magnetic imaging methods. In both cases magnetic spin-lattice relaxation is an important interpretative feature of the experiments. Although there are important and less well understood effects associated with transverse relaxation, the present discussion will be restricted to longitudinal or spin-lattice relaxation.

Relaxation coupling was treated early by Solomon who considered both heteronuclear and homonuclear coupled spin pairs (1). This work has been the foundation for a great deal of structural chemistry based on the nuclear Overhauser effect, and presently drives most large molecule structural determinations in high-field liquids NMR spectroscopy (2,3). Early magnetic resonance spectroscopy and spin relaxation studies in heterogeneous systems largely ignored the effects of magnetic coupling between the liquid spins and the solid spins, and analyses of liquid relaxation behavior were based on attempts to modify liquid models to account for possible changes in the molecular dynamics presumably associated with surfaces (4). The crucial importance

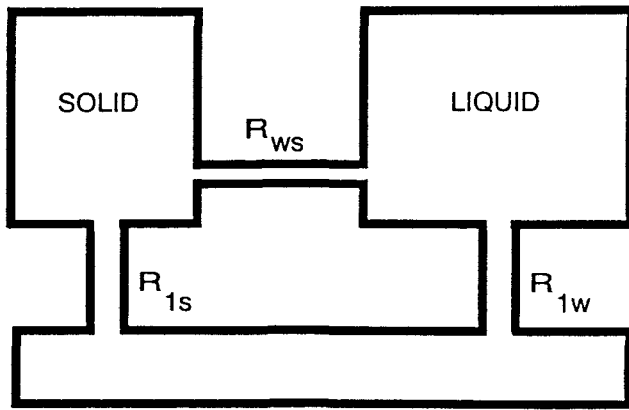


Figure 1: Schematic diagram of relaxation coupling between two coupled spin populations.

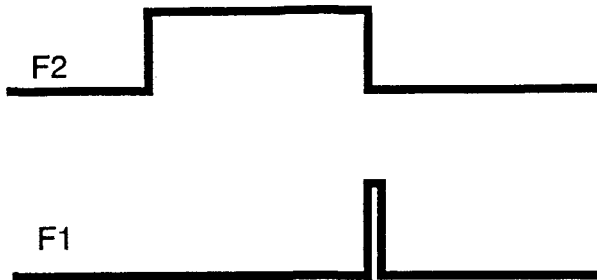


Figure 2: The pulse sequence for obtaining a Z-spectrum where the first pulse is applied at a frequency off-set from the liquid resonance frequency by  $\Delta$  and the second pulse produces a free induction decay of the liquid resonance.

of relaxation coupling between the solid and liquid spin populations was first demonstrated by Edzes and Samulski and was extended by several groups (5-13).

The crucial importance of relaxation coupling between the water spins in a tissue in determining the magnetic field dependence of spin relaxation in tissues was demonstrated first by Lester and Bryant (14,15). The use of an off-resonance presaturation pulse to control magnetic image contrast was first published by Wolf and Balaban (16), and fundamentally extended by a number of groups (17-21). We will present here the essential features of the relaxation theory, and provide examples that demonstrate the major features of the coupled systems.

The situation of two coupled spin populations, one solid and one liquid is represented schematically in Figure 1. The coupled differential equations describing this situation and their solution have been described in detail (1,5-13). The return to equilibrium of either spin population is a sum of exponen-

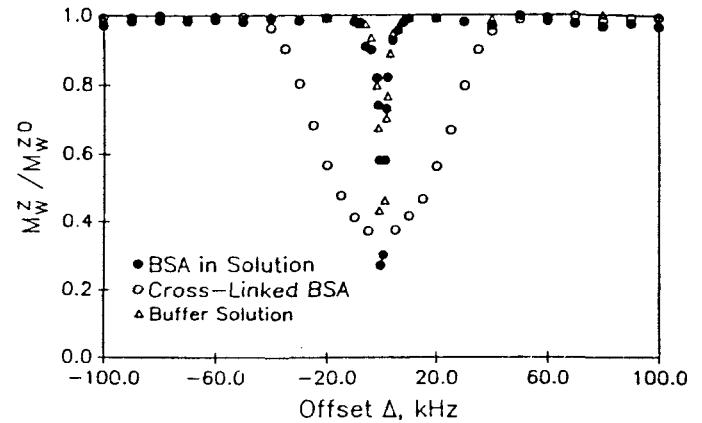


Figure 3: The normalized water proton magnetization measured at 56.4 MHz plotted as a function of the preparation pulse off-set frequency for a buffer solution, a 2 mM bovine serum albumin solution, and a cross-linked bovine serum albumin sample at ambient temperature. The preparation pulse amplitude was 0.5 kHz as was applied for 3 s.

tial growth or decay contributions with the rate constants for the slow,  $R_-$ , and fast,  $R_+$ , components given by

$$R_{\pm} = \frac{1}{2} \left\{ R_W + R_S + R_{WS} \left( 1 + \frac{1}{F} \right) \pm \left[ \left( R_S - R_W - R_{WS} \left( 1 - \frac{1}{F} \right) \right)^2 + \frac{4R_{WS}^2}{F} \right]^{\frac{1}{2}} \right\} \quad (1)$$

where  $R_W$  is the spin-lattice relaxation rate of the liquid protons in the absence of net magnetization transfer effects,  $R_S$  the spin-lattice relaxation rate of the magnetically isolated solid spin population,  $R_{WS}$  the effective transfer rate from the liquid spins to the solid spins, and  $F$  the ratio of the solid proton population to the water proton population. Although the magnitude of the effects of one population on the other clearly depend on the sizes of the two spin baths, i.e.,  $F$ , it is clear that a measurement of the relaxation of the liquid spin relaxation rate will not yield simply the relaxation rate,  $R_W$ . Further, any perturbation of one spin population will affect the other because of the coupling,  $R_{WS}$ . This observation leads to a simple but powerful experiment.

The characteristics of the solid spin spectrum are that the linewidth is typically on the order of 25-

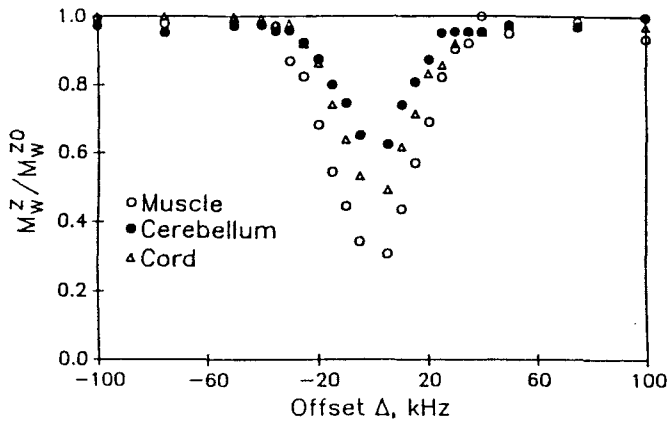


Figure 4: The normalized water proton magnetization measured at 56.4 MHz plotted as a function of preparation pulse off-set frequency for fresh rat muscle, cerebellum, and spinal cord. The preparation pulse amplitude was 0.5 kHz and was applied for 400 ms.

50 kHz and the spin-lattice relaxation rates vary depending on local dynamics in the solid, but for proteins for example, the  $T_1$  value at room temperature is on the order of 0.5 s at 60 MHz resonance frequency. Because the solid linewidth is at least a thousand times larger than the liquid component linewidth, it is possible to irradiate the solid spin population selectively and monitor the coupling into the water spin system. The simple pulse sequence to accomplish this is shown schematically in Figure 2. The preparation pulse is set off resonance from the liquid resonance usually by 10 kHz or more and left on for a duration sufficient to partially saturate the solid spin system. The second pulse applied in the center of the spectrum is nonspecific, and usually a  $90^\circ$  pulse that produces a free induction decay easily detected by a liquids spectrometer or magnetic imager. The steady-state response of the liquid magnetization following a preparation pulse at frequencies sufficiently far from the liquid resonance to avoid direct irradiation is given by

$$\frac{M_W^{SS}}{M_W^0} = 1 - \frac{2\alpha}{\beta + 4\pi^2\Delta^2\gamma}, \quad (2)$$

where

$$\alpha = \frac{FR_{SW}T_{2S}\omega_1^2}{2R_W R_S},$$

$$\beta = \frac{R_{SW}}{R_S} + F\left(\frac{R_{SW}}{R_W} + 1\right)\left(\frac{T_{2S}\omega_1^2}{R_S} + 1\right),$$

$$\gamma = T_{2S}^2\left[\frac{R_{SW}}{R_S} + F\left(\frac{R_{SW}}{R_W} + 1\right)\right]$$

$R_S$  is the spin-lattice relaxation rate of the solid-proton population in the absence of magnetization transfer,  $T_{2S}$  is the  $S$  spin-spin relaxation time,  $\Delta$  represents the offset of the preparative radio frequency field from the center of the  $S$ -spin resonance,  $\omega_1$  is proportional to the amplitude of the RF field of the preparation pulse, and  $F$  denotes the ratio of the number of  $S$  spins to the number of  $W$  spins, i.e., the water content.

This equation is not particularly transparent, but takes a familiar form in the limit of steady-state response of the liquid or water spin magnetization when the transfer rates are rapid, relative to the intrinsic relaxation rates. In this case, eqn. 2 reduces to:

$$\frac{M_W^Z}{M_W^0} = 1 - \frac{\omega_1^2 T_{1S} T_{2S}}{(1 + 4\pi^2 T_{2S}^2 \Delta^2)(1 + T_{1S}/FT_{1W}) + \omega_1^2 T_{1S} T_{2S}} \quad (3)$$

Clearly, this equation is a modified version of the usual steady-state solution of the Bloch equations for a single spin except that now there are terms resulting from the coupling of the two spin populations. The major effects of the coupling in the presence of the preparation pulse are: 1) either spin system is more difficult to saturate than it is in the absence of the relaxation coupling; 2) the liquid spin response depends on both the  $T_1$  and  $T_2$  of the solid component; 3) the magnitude of the response is a function of the ratio of the solid to liquid spin populations; and 4) the magnitude of the effect depends on the square of the rf field strength applied in the first pulse, as expected.

An example that demonstrates the importance of the dynamical state of the macromolecular components of a sample is shown in Figure 3. In this case the frequency of the preparative rf pulse is varied systematically over a 100 kHz range either side of the central water resonance in an aqueous protein solution and in the same solution after it

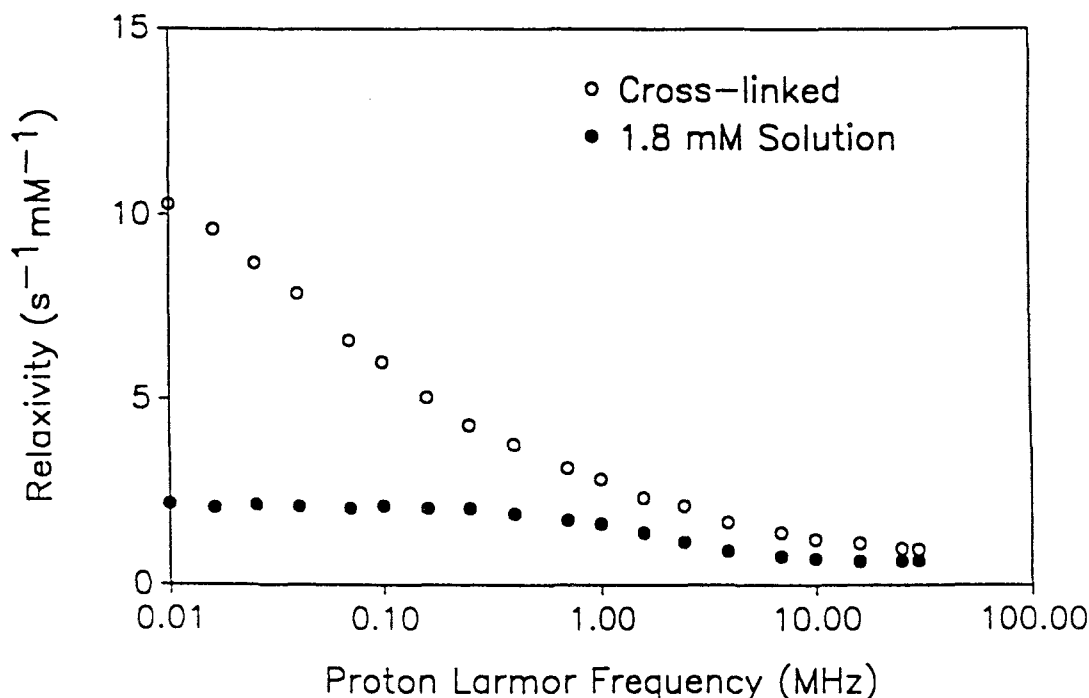


Figure 5: The water proton spin-lattice relaxation rate measured as a function of magnetic field strength reported as the proton Larmor frequency at 298 K for a 1.8 mM bovine serum albumin sample. The lower curve was obtained on the solution (filled circles), the upper curve was obtained after the solution was cross-linked with glutaraldehyde to stop the rotational motion of the protein (open circles).

is chemically cross-linked to stop rotational motion of the protein. The vertical axis of the plot is the normalized water resonance intensity, i.e., the water peak amplitude in the experiment divided by the water peak amplitude when the preparative pulse is very far from the water resonance frequency. The horizontal axis is the frequency offset of the preparative pulse from the water resonance frequency. We have called this presentation a Z-spectrum because it represents the response of the liquid Z-magnetization to perturbation of the solid component Z-magnetization.

Inspection of Figure 3 shows that there is little effect of the off-resonance pulse on the water resonance in the concentrated protein solution, and the decline in the water resonance intensity results only when the water resonance is directly irradiated. However, when the protein rotational motion is stopped by the introduction of chemical cross-links so that a gel results, the protein proton spectrum becomes that characteristic of a solid with about a 35 kHz linewidth and the water resonance responds dramatically to the off-resonance preparation pulse. As Figure 3 shows, a map of the solid proton spec-

trum is obtained by observation of the water proton spectrum. As eqn. 3 shows, this representation of the solid spectrum may be broadened, depending on the level of the rf field used in the preparation pulse; however, the experiment provides a very simple way to obtain an accurate NMR spectrum of solid components without the usual dead-time problems if one extrapolates to minimal rf amplitude of the preparation rf pulse. The data in Figure 4 show that the experiment works well in the context of animal tissues and that not all tissues respond identically. The differences from one tissue to another may result from differences in the solids/liquids ratio or the water content, as well as from differences in the solid relaxation times that enter the relaxation equation. In any case, a simple strategy for utilizing this experiment in an imaging context is apparent. That is, prior to the imaging sequence, execute a single preparation pulse perhaps 10 kHz or more off resonance from the water signal, which will partially saturate some of the solid components depending on their local dynamics. In turn the water magnetization will respond because of the cross-relaxation term in the relaxation equation, and the

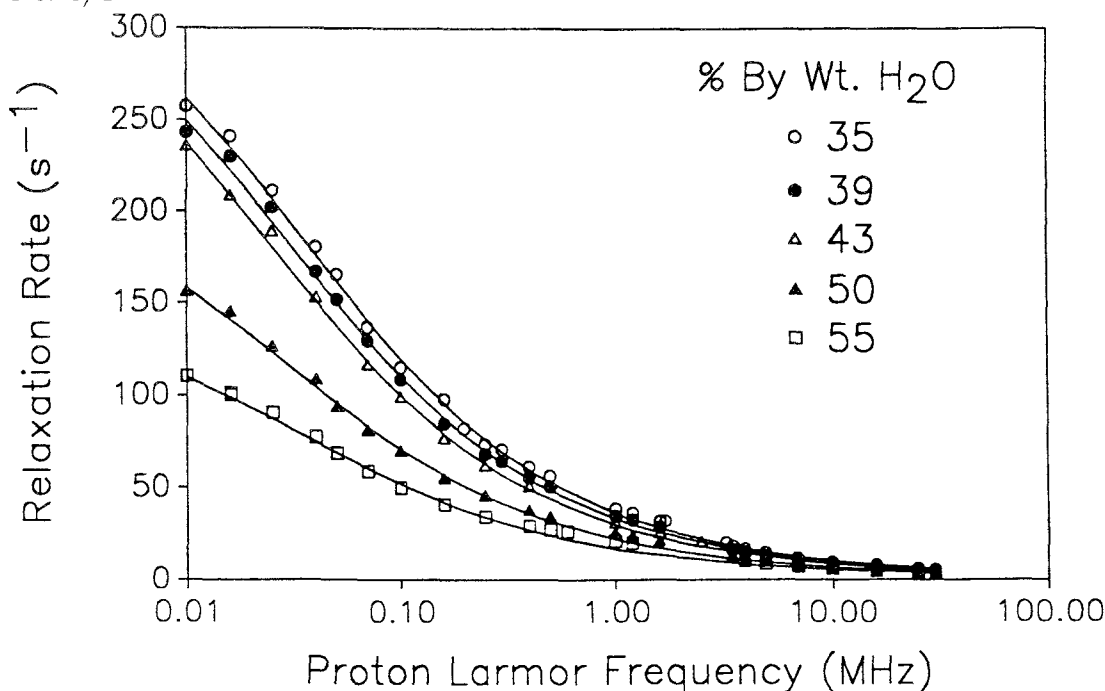


Figure 6: The water proton spin-lattice relaxation rates as a function of magnetic field strength reported as the proton Larmor frequency in hydrated lysozyme at 291 K. The levels of water content are expressed as the ratio of the weight of water to the total weight of the sample. The solid lines are fits to the solution of the coupled relaxation equations slow component with the magnetic field dependence of the solid component given by the power law dependence discussed in the text.

water magnetization will drop. The resulting image will now produce intensities that are determined in large measure by the relaxation properties of the solid components of the sample. From a medical point of view, the key issue is whether this approach will detect significant changes in a tissue as a consequence of pathological development. Clearly, in some cases this is expected to be true. Many tumors are palpable lumps readily detected within the host tissue. Therefore, there must be within these structures additional macromolecular components that are more rigid than those of the host tissue, and the Z-spectrum as well as the magnetic image obtained following the off-resonance preparation pulse should show this change that may affect  $F$  as well as the relaxation parameters of the solid system.

Magnetic coupling between the liquid and solid components of a heterogeneous material is fundamental to understanding the magnetic field dependence of the spin-lattice relaxation rate. The results of a key experiment are shown in Figure 5. The relaxation dispersion of a concentrated protein solution shows an inflection at proton Larmor frequencies that correspond to the frequencies of the rotational motion of the protein. However, when

the system is cross-linked at constant composition, the relaxation dispersion profile changes profoundly; the approximately Lorentzian character of the relaxation profile is lost, and a power-law dependence is observed. The effect of the magnetic coupling between the liquid and solid components is to transfer the magnetic field dependence of the rotationally immobilized components to the proton relaxation of the liquid. The magnetic field dependence of the dry protein has been reported (22) by Kimich and coworkers who find that the relaxation rate depends on  $\nu_{-B}$  where  $B$  is approximately 0.74. The hydrated system shown in Figure 5 as well as those shown in Figure 6 are better fit with  $B = 0.57$ . In either case, the magnetic field dependence of the protein is related to the internal fluctuations of the rotationally immobilized protein molecules. The magnetic cross-relaxation between the liquid and the solid components of the heterogeneous material transfers the magnetic field dependence of the solid components to the liquid components and results in the same shape, scaled by the ratio of the populations.

Using the solution of the coupled relaxation equations, eqn. 1, Lester and Bryant (31) were able

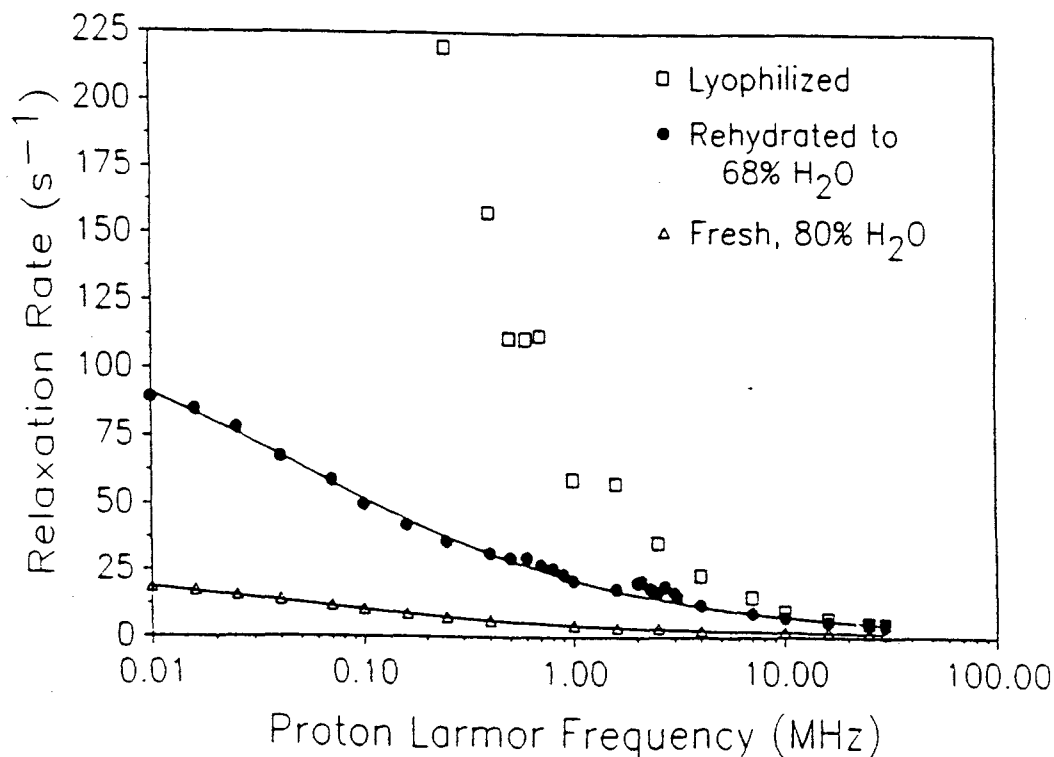


Figure 7: The water proton spin-lattice relaxation rate measured as a function of magnetic field strength reported as the proton Larmor frequency at 291 K for rat cerebral cortex fresh and containing 80% water by weight, lyophilized and dry, and rehydrated to a water content of 68% by weight. The solid lines were computed from the coupled relaxation model.

to model the water content dependence of the relaxation dispersion profiles in hydrated lysozyme as shown in Figure 6. Similar results were obtained when the water content was changed in the more complicated tissue system as shown in Figure 7. In summary, the magnetic field dependence of the water proton relaxation rate in tissues and other heterogeneous systems may be explained by the coupling scheme of Figure 1, where the magnetic field dependence is contained in the parameters of the solid spin system, and transferred to the liquid by the cross-relaxation pathway.

The nature of the relaxation coupling poses an interesting question because both chemical exchange of labile proton on the solid matrix and dipole-dipole couplings may contribute to the effective magnetization transfer between the liquid and the solid. Although this issue may have no uniformly valid answer because the chemical exchange contributions are undoubtedly a function of pH, temperature, and the character of the solid matrix, one experiment which demonstrates that chemical exchange is

not an obligatory component of the magnetization transfer was published by Grad and Bryant and is shown in Figure 8. The essence of this experiment is that the methyl protons of the dimethyl sulfoxide are not labile and will not exchange chemically between the methyl groups of the solvent and the protein. On the other hand, the water protons are labile and may exchange between the water molecule and ionizable functions on the protein such as ammonium ions, OH groups, amides, etc. Nevertheless, the observed Z-spectrum of the DMSO protons and the water proton are essentially identical which means that while the chemical exchange may contribute to the water Z-spectrum, the effect may also be carried only by the dipole-dipole coupling. Thus, the applications of Z-spectroscopy or the imaging versions of the experiment are not limited to liquids like water with labile protons.

In summary, the relaxation coupling between liquid and solid components of a heterogeneous material provide both problems and opportunities. The readily observed relaxation behavior is not accu-

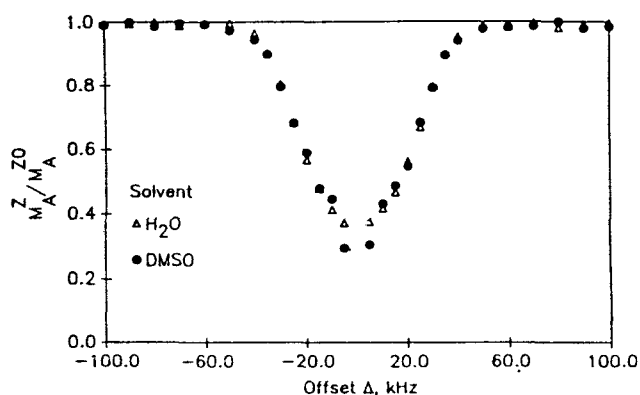


Figure 8: The Z spectra of cross-linked bovine serum albumin gels obtained by observing the water proton and the methyl protons of dimethylsulfoxide. These spectra were obtained using a recycle delay time of 5 s, a preparation pulse duration of 3 s at an rf level of 0.5 kHz.

rately interpreted using the usual relaxation equations appropriate for liquids. On the other hand, the liquid spin system may provide considerable information about the character of the solid components which provide particularly interesting opportunities for new applications in diagnostic medical imaging. The obvious application of coupled relaxation methods is to change image contrast so that pathological changes may be better visualized without the need for introducing specific contrast agents. However, as discussed above, the response of the liquid components of the system to the characteristics of the solid may provide a means for changing the information content of the magnetic image; that is, to characterize the normally invisible components of the system by observation of the liquid signals. It remains to be learned whether these new data will provide non-invasive diagnostic resolution of presently confusing imaging presentations.

### III. Acknowledgments

This work was supported by the National Institutes of Health, GM34541 and GM39309, The University of Rochester and the University of Virginia. The author acknowledges with pleasure the considerable contributions to this field by former students, particularly Jonathan Grad and Cathy Coolbaugh Lester. This manuscript was presented as part of the Waterloo Summer School, University of Waterloo, Water-

loo, Ontario, Canada in the summer of 1993. Since this time, several important contributions have been made by several groups including those of Balaban, Glover, Henkelman, Koenig, Schleich, Swanson, Yeung, Wu, and the present author. There are improved theoretical descriptions of the Z-spectrum lineshape which more correctly treats the solid spin lineshape. Nevertheless, the fundamental features of the experiment and its analytical utility remain as summarized here. Extensive applications of the approach have been made in clinical magnetic resonance imaging.

### IV. References

- <sup>1</sup>I. Solomon, *Phys. Rev.* **99**, 559 (1955).
- <sup>2</sup>J. H. Noggle and R. E. Schirmer, "The Nuclear Overhauser Effect, Chemical Applications," Academic Press, New York, 1971.
- <sup>3</sup>K. Wuthrich, "NMR of Proteins and Nucleic Acids," Wiley, New York, 1986.
- <sup>4</sup>H. Resing, *Adv. Mol. Relax. Processes* **3**, 199 (1972).
- <sup>5</sup>A. Kalk, H. J. C. Berendsen, *J. Magn. Reson.* **24**, 343 (1976).
- <sup>6</sup>H. T. Edzes, E. T. Samulski, *Nature* **265**, 521 (1977).
- <sup>7</sup>H. T. Edzes, E. T. Samulski, *J. Magn. Reson.* **31**, 207 (1978).
- <sup>8</sup>E. Hsi, R. G. Bryant, *Arch. Biochem. Biophys.* **183**, 588 (1977).
- <sup>9</sup>S. H. Koenig, R. G. Bryant, K. Hallenga, G. S. Jacobs, *Biochemistry* **17**, 4348 (1978).
- <sup>10</sup>B. M. Fung, T. W. McGaughy, *J. Magn. Reson.* **31**, 413 (1980).
- <sup>11</sup>W. E. Shirley, R. G. Bryant, *J. Am. Chem. Soc.* **104**, 2910 (1982).
- <sup>12</sup>J. C. Gore, M. S. Brown, J. Zhong, K. F. Mueller, W. Good, *Magn. Reson. Med.* **9**, 325 (1989).
- <sup>13</sup>J. C. Gore, M. S. Brown, I. M. Armitage, *Magn. Reson. Med.* **9**, 333 (1989).
- <sup>14</sup>C. C. Lester, R. G. Bryant, *Magn. Reson. Med.* **22**, 143 (1991).
- <sup>15</sup>R. G. Bryant, D. A. Mendelson, C. C. Lester, *Magn. Reson. Med.* **21**, 117 (1991).
- <sup>16</sup>S. D. Wolf, R. S. Balaban, *Magn. Reson. Med.* **10**, 135 (1989).

<sup>17</sup>J. Grad and R. G. Bryant, *J. Magn. Reson.* **90**, 1 (1990).

<sup>18</sup>H. N. Yeung and S. D. Swanson, *J. Magn. Reson.*, in press.

<sup>19</sup>X. Wu, *J. Magn. Reson.* **94**, 186 (1991).

<sup>20</sup>G. H. Caines, T. Schleich, J. M. Rydzewski, *J. Magn. Reson.* **95**, 558 (1991).

<sup>21</sup>S. D. Swanson, *J. Magn. Reson.* **95**, 615 (1991).

<sup>22</sup>R. Kimmich, F. Winter, W. Nusser, K.-H. Spohn, *J. Magn. Reson.* **68**, 263, (1986).